Heliyon 9 (2023) e22151

Contents lists available at ScienceDirect

Heliyon

journal homepage: www.cell.com/heliyon

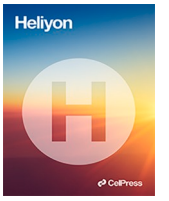

Comparative analysis of the synergetic effects of Diwuyanggan prescription on high fat diet-induced non-alcoholic fatty liver disease using untargeted metabolomics

Jinlin Xu [a,b,1], Yuehui Jin [a,1], Chengwu Song [a,1], Guangya Chen [b], Qiaoyu Li [a], Hao Yuan [a,b], Sha Wei [c], Min Yang [c], Sen Li [d,**], Shuna Jin [c,*]

[a] School of Pharmacy, Hubei University of Chinese Medicine, Wuhan 430065, China
[b] Department of Pharmacy, Ezhou Central Hospital, Ezhou 436000, China
[c] School of Basic Medicine Sciences, Hubei University of Chinese Medicine, Wuhan 430065, China
[d] Department of Pharmacy, Union Hospital, Tongji Medical College, Huazhong University of Science and Technology, Wuhan 430030, China

ARTICLE INFO

Keywords:
Diwuyanggan
Non-alcoholic fatty liver disease
Metabolomics
Disassembled prescriptions
Combination mechanism
LC-MS/MS

ABSTRACT

Non-alcoholic fatty liver disease (NAFLD) is one of the most common chronic liver disorders worldwide and had no approved pharmacological treatments. Diwuyanggan prescription (DWYG) is a traditional Chinese medicine preparation composed of 5 kinds of herbs, which has been used for treating chronic liver diseases in clinic. Whereas, the synergistic mechanism of this prescription for anti-NAFLD remains unclear. In this study, we aimed to demonstrate the synergetic effect of DWYG by using the disassembled prescriptions and untargeted metabolomics research strategies. The therapeutic effects of the whole prescription of DWYG and the individual herb were divided into six groups according to the strategy of disassembled prescriptions, including DWYG, *Artemisia capillaris* Thunb. (AC), *Curcuma longa* L. (CL), *Schisandra chinensis* Baill. (SC), *Rehmannia glutinosa* Libosch. (RG) and *Glycyrrhiza uralensis* Fisch. (GU) groups. The high fat diets-induced NAFLD mice model was constructed to evaluate the efficacy effects of DWYG. An untargeted metabolomics based on the UPLC-QTOF-MS/MS approach was carried out to make clear the synergetic effect on the regulation of metabolites dissecting the united mechanisms. Experimental results on animals revealed that the anti-NAFLD effect of DWYG prescription was better than the individual herb group in reducing liver lipid deposition and restoring the abnormality of lipidemia. In addition, further metabolomics analysis indicated that 23 differential metabolites associated with the progression of NAFLD were identified and 19 of them could be improved by DWYG. Compared with five single herbs, DWYG showed the most extensive regulatory effects on metabolites and their related pathways, which were related to lipid and amino acid metabolisms. Besides, each individual herb in DWYG was found to show different degrees of regulatory effects on NAFLD and metabolic pathways. SC and CL possessed the highest relationship in the regulation of NAFLD. Altogether, these results provided an insight into the

* Corresponding author.
** Corresponding author.
E-mail addresses: xujinlin802@163.com (J. Xu), jinyuehui21@outlook.com (Y. Jin), chengwusong_2016@hbtcm.edu.cn (C. Song), qq767586330@163.com (G. Chen), qiaoyuli_hzy@163.com (Q. Li), yuanh4399@163.com (H. Yuan), weisha2021@hbtcm.edu.cn (S. Wei), yangmin2021@hbtcm.edu.cn (M. Yang), lisentome728@hotmail.com (S. Li), jinshuna2021@hbtcm.edu.cn (S. Jin).
[1] These authors contributed equally to this article.

https://doi.org/10.1016/j.heliyon.2023.e22151
Received 17 July 2023; Received in revised form 3 November 2023; Accepted 5 November 2023
Available online 10 November 2023

synergetic mechanisms of DWYG from the metabolic perspective, and also supported a scientific basis for the rationality of clinical use of this prescription.

1. Introduction

Non-alcoholic fatty liver disease (NAFLD) is distinguished by overaccumulation of fat in the absence of excess alcohol consumption or other liver disorders [1]. NAFLD is typically a progressive disease that can be associated with grievous complications like nonalcoholic steatohepatitis, hepatocirrhosis and hepatocellular carcinoma, as well as increased liver-related mortality [2,3]. It is one of the most frequent chronic liver diseases in the developed world, affecting approximately a quarter of the global population [4]. Currently, there was no pharmacotherapy approved for this disease to date due to the complexity of NAFLD.

Traditional Chinese medicine (TCM) prescriptions are normally used with the combination of multiple herbs [5]. The resulting mixture of herbs follows the principle of combined utilization that implies maximization of the efficacy and minimization of the adverse reactions, which in turn may explain the widely use of TCM in the first-line clinical application [6,7]. Diwuyanggan (DWYG) is a TCM prescription mainly used to treat chronic liver diseases clinically which could delay or even reverse the progression of chronic hepatitis B, liver fibrosis and liver cancer [8–11]. DWYG contains five herbs: the aerial part of *Artemisia capillaris* Thunb. (Yin-Chen), the rhizome of *Curcuma longa* L. (Jiang-Huang), the fruit of *Schisandra chinensis* Baill. (Wu-Wei-Zi), the steamed roots of *Rehmannia glutinosa* Libosch. (Shu-Di-Huang), the roots of *Glycyrrhiza uralensis* Fisch. (Gan-Cao). In our previous studies, DWYG was found to have a preventive effect on acute liver injury [12]. Up to now, quite a few pharmacological experimental studies have indicated that five herbs in DWYG have hepatoprotective effect alone [13–17], but the synergetic mechanisms of DWYG remain unclear enough in NAFLD prophylaxis and treatment.

Despite the role of TCMs and their combination in pharmacodynamics can be understood through conventional animal experiments [18]. However, it is hard to dissect the combination mechanisms because TCM has multi-component and multi-target features, as well as possesses a complex in vivo interaction [19]. Therefore, we decomposed the prescription into individual drugs, which is one of the most generally used approaches to research the combined utilization rules of TCM at present [20]. By using this way, such an analysis strategy would contribute to the discovery of the relationship between single drug and DWYG formula and clarify the synergetic effects of DWYG. In the last decade, with the continuous development of multiple analytical platforms, metabolomics has been used to decipher the mystery of TCM synergy [21,22]. Metabolomics studies the overall state of biological systems and the endogenous metabolites changes in the whole organism for the purpose of elucidating the mechanism of drug action in the body, with an emphasis on globality and dynamics [23,24]. The characteristics of metabolomics are similar to the holistic view of the TCM theory, making it an effective approach to clarify the combined use of TCM prescriptions and the modernization of TCM [25]. Besides, ultra-high-pressure liquid chromatography combined with quadrupole time-of-flight mass spectrometry (UPLC-QTOF-MS/MS) has been recognized as a suitable metabolomic tool due to its high resolution, which provides accurate mass [26,27]. Therefore, using the metabolomics research method based on UPLC-QTOF-MS/MS, the differences in the regulatory indicators of the five herbs could be compared after dismantling prescriptions into single herbs, and synergetic effects of TCM formulas could be explained.

In this study, the efficacy effects of DWYG and its five individual herbs on the treatment of high fat diets (HFD)-induced NAFLD were evaluated. Then, a strategy combining metabolomics and disassembled prescriptions was employed to analyze the synergy rules of TCM prescriptions. Further, the differences in the therapeutic mechanisms of DWYG and its single herbs for the treatment of NAFLD were analyzed by metabolic pathways. These findings will provide a theoretical foundation for clarifying the scientific connotations of the synergetic mechanism of DWYG prescription.

2. Materials and methods

2.1. Chemicals and reagents

All of the raw herbal medicines were supplied by the TCM Preparation Room of Hubei Provincial Hospital of TCM and authenticated in Hubei University of Chinese Medicine. HPLC grade acetonitrile were obtained from Fisher Scientific (Fair Lawn, NJ, USA). Water was purified using a Milli-Q super purification system from Millipore (Millipore, Bedford, MA, USA). Formic acid (≥98 %) of analytical grade was purchased from Sinopharm Chemical Reagent Co., Ltd (Shanghai, China). The standards of puerarin (≥98 %) was purchased from Aladdin (Shanghai, China). Simvastatin was purchased from Shanghai yuanye Bio-Technology Co., Ltd (Shanghai, China). TC (total cholesterol), HDL-C (low-density lipoprotein cholesterol), LDL-C (high-density lipoprotein cholesterol) assay kits (batch number: 20211220, 20210514 and 20211220, respectively) were obtained from Nanjing Jiancheng Bioengineering Institute (Nanjing, China).

2.2. Preparation of herbs extracts

DWYG includes five herbal extracts in proportion with (w/w) *Schisandra chinensis* Baill., 20.0 %; *Curcuma longa* L., 13.4 %; *Artemisia capillaris* Thunb., 33.3 %; *Rehmannia glutinosa* Libosch., 20.0 %; *Glycyrrhiza uralensis* Fisch., 13.4 %. The coarse powder of *Schisandra chinensis* Baill. and *Curcuma longa* L. were extracted 3 times with 70 % ethanol (1:2.23, 1:1.61, 1:1.61 w/v) for 1 h. The other three herbs were decocted 3 times with boiling water (1:6, 1:3, 1:3 w/v) for 1.5 h. The ethanol and water extracts were mixed after being

filtered with gauze, and the merged mixtures were concentrated and then dried under vacuum, ground into powder. The above process followed the production standard of DWYG Capsules at Hubei Province Hospital of TCM. The preparation process of five single herbal extracts was identical to that of DWYG. All herbal extracts were stored at −20 °C.

2.3. Animal experiments

Eighty-eight male Kunming mice, weighing 20–25 g, were purchased from the Animal Center of Tongji Medical College, Huazhong University of Science and Technology (Wuhan, China), approval No. SCXK (e) 2017- 0067. All mice were housed in a standard animal laboratory at 24 ± 2 °C (temperature), 60 ± 5 % (humidity) and 12 h light-dark photoperiod. HFD were prepared in the following proportions: standard diet (78.8 %), lard (10 %), egg yolk (10 %), cholesterol (1 %), and cholate (0.2 %) [28]. We followed the requirements of the Animal Ethics Committee of Hubei University of Chinese Medicine for all animal procedures (approval number: 202203004).

After a week of acclimatization, they were stochastically partitioned into nine groups: Control group (C group), NAFLD model group (M group), Positive drug group (P group), Artemisia capillaris Thunb group (AC group), Curcuma longa L group (CL group), Schisandra chinensis Baill group (SC group), Rehmannia glutinosa Libosch group (RG group), Glycyrrhiza uralensis group (GU group), DWYG group (DW group). There were ten mice in each group, except for 8 mice in the P group. Except for those in the C group, all mice were received HFD to induce NAFLD for 5 weeks. Then, the mice in the P group were given simvastatin at a dose of 40 $mg{\cdot}kg^{-1}$, and the mice in the AC, CL, SC, GU and DWYG groups were given their corresponding extracts once a day intragastrically at doses of 150 $mg{\cdot}kg^{-1}$. Meanwhile, 0.4 mL of distilled water was given to the C and M groups in the same manner.

After 5 weeks of feeding along with 4 weeks of continuous intragastric administration, the mice were supplied with water for 12 h but were deprived of food. Then, during pentobarbital sodium anesthesia, the blood samples of all the mice were collected by enucleating their eyeball. After 30 min standing time at ambient temperature, the serum was centrifuged for 15 min at 2680 g and kept at −80 °C for standby.

Serum TC, LDL-C, and HDL-C were assayed using commercial kits. Meanwhile, liver tissues from each animal were excised immediately, washed with cold saline, and weighed. Portions of those were fixed in 4 % tissue fixation solution, and stained with Oil Red O for histological examination. The hepatic index was calculated by means of the following formula: Hepatic index = (liver weight/body weight) × 100 %.

2.4. Sample preparation

160 μL of acetonitrile was added to 40 μL of thawed serum samples. Subsequently, 50 μL puerarin solution as an internal standard with concentrations of 500 $ng{\cdot}mL^{-1}$ was pipetted into each sample, followed by 5 min for vortexing. The mixture was then placed at 4 °C for 10 min, centrifuged at 12830 g at 4 °C for 10 min to remove the precipitated proteins. Finally, prior to LC-MS/MS analysis, 150 μL of supernatant was carefully transferred to sample vials and refrigerated at −20 °C. To guarantee the stability and repeatability of LC-MS system, the quality control samples (QC) were obtained by mixing the same volume of serum from each sample and inserted every 5 samples throughout the whole sequence analysis.

2.5. UPLC-QTOF-MS/MS conditions

A Waters ACQUITY UPLC M-Class system was used for serum metabolic profiling analysis. For chromatographic separation, a 2.0 μL aliquot of the supernatant was injected into system at 40 °C on a Waters ACQUITY UPLC BEH C18 column (2.1 × 100 mm, 1.7 μm). At a flow rate of 0.3 mL min^{-1}, the mobile phase of the eluent consisted of water-formic acid (1000:1, v/v) (A) and acetonitrile (B). The mobile phase was delivered using the following linear gradient: 0 min, 10 % B; 15.0 min, 95 % B; 20.0 min, 95 % B; 21.0 min, 10 % B; 25.0 min, 10 % B.

Mass spectrometry was carried out using a Waters Xevo G2-XS QTof system equipped with an electrospray ion source (Waters, Mass., USA), in which the positive and negative ion modes were set with sensitivity analysis modes. The specific conditions of MS were as follows: desolvation and source temperature of 500 °C and 100 °C; desolvation and cone gas flow of 600 $L{\cdot}h^{-1}$ and 50 $L{\cdot}h^{-1}$; capillary and cone voltage of 3000 V and 60 V. The mass data was acquired in the range of mass-to-charge ratio (m/z) 50 to 1200 Da in MS^E mode. And the full scan duration time was set to 0.5 s.

2.6. Data processing and statistics analysis

The raw files were acquired using MassLynx software (Waters Corporation, Milford, MA, USA). Markerlynx XS (Waters, Mass., USA) was applied to perform noise filtering, isotope peak exclusion, peak extraction, peak alignment and area normalization. The data processing parameters were set as follows: the mass tolerance of 0.01 Da was set for peak alignment; the retention time for the peak extraction was set from 2 min to 20 min; the noise elimination level was set at 50. As a result, the visual data matrix was generated, which included retention time, m/z, sample information, and each feature's intensity. After filtering the features based on the 60 % rule, the data was transformed into decimal logarithms (log10 transformation), to address missing value input and reduce skewness in the distribution.

The resultant data matrices (Table S1) were then imported to SIMCA-P 14.1 software (Umetrics, Umea, Sweden) for the purpose of multivariate analysis. Unsupervised principal component analysis (PCA) as an unsupervised dimensionality reduction model was

applied for visualize data with clustering analysis of samples. Subsequently, to evaluate metabolic alterations among all the groups, orthogonal partial least squares-discriminant analysis (OPLS-DA) was performed. Furthermore, using 999 response permutation testing (RPT), a validation for the quality of the OPLS-DA model was achieved by means of computing R^2 and Q^2 values. Variable importance in projection (VIP) scores were calculated for determining the key metabolite, and those metabolites with VIP >1.0 were considered statistically significant [29]. VIP values of the OPLS-DA model greater than 1.0 between the C group and M group were selected for further analysis. The fold change (FC) values referred to the ratio of the mean abundances of metabolites between any two groups, and was another factor for screening variables, used as a measure to explain how much a quantity changes going from a starting to a final value. Metabolites with a VIP greater than 1 that met one of the following two criteria were considered to be potential biomarkers. First, the contents of metabolites had significant differences (P value < 0.05) calculated by Mann-Whitney U test using IBM SPSS Statistics 26.0 (SPSS Inc., Chicago, Illinois, USA). The other was the ratio of the average content of metabolites was FC $\geq$ 1.1or FC $\leq$ 0.9.

Metabolites were identified by matching MS/MS fragmentation ion characteristics in the METLIN database (http://metlin.scripps.edu) and Human Metabolome Database (https://www.hmdb.ca) with ±20 ppm tolerance. A heat map was generated to depict the relative differences in the metabolites found in each group using GraphPad Prism 9.0 (GraphPad Software Inc., San Diego, CA). Then, the potential biomarkers were mapped to the reference paths against the KEGG Database (https://www.kegg.jp). Finally, the Cytoscape 3.8.2 software (https://cytoscape.org) was performed to assist in elucidating the synergistic effects of DWYG by constructing a network.

3. Results

3.1. Prevention and treatment of DWYG and its single drug on HFD-induced NAFLD

As shown in Table 1, the body weights, liver weights, hepatic indexes, TC, HDL-C, and LDL-C in each group were conducted. After 5 weeks of experimentation, compared to C group, the body weights, hepatic indexes, TC, HDL-C, and LDL-C of mice with HFD changed obviously. The above data in combination with the liver morphology and histopathology indicated that NAFLD model was successfully established. However, the liver weights and hepatic indexes of mice treated with SC and DW have a significant improvement. Compared to the model group, all the treatment groups for body weight had some amelioration with no remarkable change, but to varying degrees, except RG. In addition, the results of serum TC values showed that AC, CL, SC, GU, DW significantly decreased in comparison to M group, and the decrease ratio of them were 17.26 %, 14.12 %, 15.55 %, 22.11 % and 17.97 %, respectively. Meanwhile, the values of HDL-C in all administered groups were prominently decreased in comparison to the M group. Concerning the serum LDL-C level of mice, P, AC, CL, SC, RG, GU and DW inhibited the elevation of LDL by 44.44 %, 33.33 %, 20.37 %, 25.00 %, 33.33 %, 46.30 % and 50.00 % respectively, and all administered groups except CL had a significant reduction compared to the model mice ($P < 0.01$, $P < 0.001$). All of these results demonstrated that simvastatin, DWYG and its single herbal groups have different degrees of amelioration in fat accumulation in the liver compared to the model group. Especially, the comprehensive effect of DWYG showed better improvement on fatty liver than five single herbal groups and positive drug group.

The results of the morphological and histopathological analysis of liver tissues were depicted in Fig. 1. In Fig. 1A, HFD was successful in causing severe fatty liver after treatment for 5 weeks, which performed for the liver felt oily, with a tawny and swollen surface. Besides, the morphological changes were not obvious for the AC, CL, SC, RG, CU and DW groups, whose treatment effects were better ameliorated than the positive group. As shown in Fig. 1B, the liver histopathology observation suggested the livers in C group showed normal histological structure, and a radial distribution of hepatocytes surround the central vein. And, the livers in M group exhibited fewer nuclei, eccentric nuclei, hepatocyte ballooning, and lipid deposition. Conversely, after 4 weeks' treatment of herbal

Table 1
Characteristics of NAFLD mice with DWYG and its single herb treatment for 4 weeks (mean ± SD).

Group	Physical parameters			Biochemical parameters of serum		
	body weight (g)	liver weight (g)	Hepatic indexes (%)	TC (mmol/L)	HDL-C (mmol/L)	LDL-C(mmol/L)
C (n = 10)	47.13 ± 4.16*	1.95 ± 0.38	4.11 ± 0.54*	5.07 ± 1.21***	4.77 ± 1.16***	0.29 ± 0.07***
M (n = 10)	50.91 ± 5.13	2.35 ± 0.29	4.63 ± 0.50	7.01 ± 0.83	3.32 ± 0.68	1.08 ± 0.18
P (n = 8)	49.40 ± 5.44	2.33 ± 0.48	4.70 ± 0.56	6.89 ± 1.10	3.77 ± 0.60*	0.60 ± 0.20***
AC (n = 10)	48.25 ± 3.47	2.12 ± 0.16	4.39 ± 0.29	5.80 ± 1.44*	4.11 ± 1.33*	0.72 ± 0.25***
CL (n = 10)	47.15 ± 4.31	2.15 ± 0.36	4.57 ± 0.72	6.02 ± 1.60*	4.32 ± 1.39*	0.86 ± 0.29
SC (n = 10)	49.38 ± 3.61	1.98 ± 0.25**	4.02 ± 0.42**	5.92 ± 0.78*	4.24 ± 1.10*	0.81 ± 0.17**
RG (n = 10)	52.68 ± 4.97	2.18 ± 0.41	4.14 ± 0.60	6.20 ± 0.73	4.20 ± 0.67**	0.72 ± 0.17**
GU (n = 10)	47.32 ± 3.76	2.15 ± 0.27	4.54 ± 0.45	5.46 ± 1.61**	3.76 ± 1.06*	0.58 ± 0.21***
DW (n = 10)	47.64 ± 3.85	1.96 ± 0.28**	4.10 ± 0.42**	5.75 ± 0.54**	4.71 ± 0.92***	0.54 ± 0.07***

Abbreviation: TC, total cholesterol; LDL-C, low-density lipoprotein cholesterol; HDL-C, high-density lipoprotein cholesterol; Hepatic indexes= (liver weight/body weight) × 100 %.

N: normal group; M: NAFLD model group; P: positive group; AC: Artemisia capillaris Thunb treatment group; CL: Curcuma longa L treatment group; SC: Schisandra chinensis Baill treatment group; RG: Rehmannia glutinosa Libosch treatment group; GU: Glycyrrhiza uralensis treatment group; DW: Diwuyanggan treatment group.

*$P < 0.05$, **$P < 0.01$, ***$P < 0.001$, significantly different from group M.

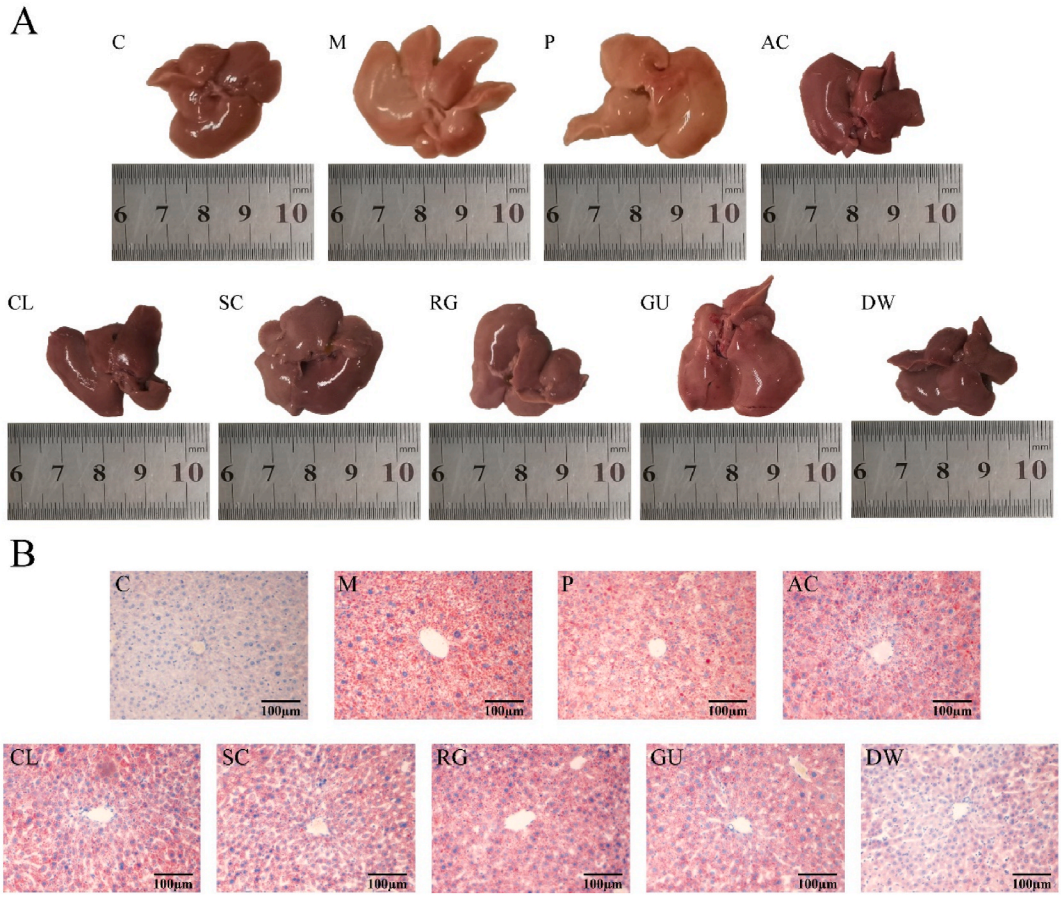

Fig. 1. The effect of each group on the histopathology of liver tissue. **A:** Morphology of liver from each group; **B:** Representative photomicrograph of liver histology (Oil Red-O staining, magnification 100 ×).

extracts, there was a trend of relative amelioration in the degree of liver steatosis in mice. Meanwhile, NAFLD mice treated with DWYG, showed a close morphology restitution to normal. In conclusion, it was further confirmed that DWYG composed of AC, CL, SC, RG and GU could effectively attenuate the fat accumulation as well as inhibit hepatic steatosis development in mice induced by HFD.

3.2. Serum metabolic profile analysis

3.2.1. Identification and quantitative analysis of potential serum biomarkers

Metabolomics analysis by UPLC-QTOF-MS/MS was performed on serum from mice of eight groups (C, M, AC, CL, SC, RG, GU, and DW). Representative total ion chromatograms (TIC) of serum samples were displayed in Figs. S1A–S1H. To investigate metabolic profiles, PCA was performed among 9 groups for the serum samples with the results of $R^2X = 0.194$, $Q^2 = 0.160$. It can be seen from Fig. 2A that the aggregation trend of each group was obvious, there was a clear separation between the C group and M group, as well as among the M group and all the TCM intervention groups. The results indicated that the NAFLD pathological process caused by HFD changed in endogenous metabolites, and the administration of herbal extracts could change the serum metabolic profile of mice in M group. However, there was considerable overlap of TCM intervention groups, resulting in relatively low explanation of PCA model. Meanwhile, well gathering QC samples near the ellipse center, indicated reliable stability of the analytical method. In order to evaluate the difference of metabolic information among five single herbs administered groups and DWYG prescription administered group, a PCA model was constructed ($R^2X = 0.316$, $Q^2 = 0.124$), as shown in Fig. 2B. Similarly, DWYG group clustered considerable overlap to CL and SC groups, which indicated that mice exposed to CL, SC showed similar metabolic phenotypes to DWYG prescription.

For further study, a supervised OPLS-DA model was developed for the discovery of potential markers for the NAFLD pathological process and the treatment of DWYG on mice. As depicted in Fig. 2C, the R^2Y and Q^2 values of OPLS-DA model were 0.990 and 0.849, which suggested the excellent fitting and prediction dependability. In the meantime, permutation test for 999 iterations was negative for Q^2, indicating model of OPLS-DA were not random and overfitted (Fig. 2D). And the OPLS-DA score plots and the corresponding 999 permutation tests of the control, model, and intervention groups were shown in Figs. S2A–S2F and Figs. S3A–S3F. The results indicated that all models were similarly reliable and not overfitted.

According to the selection criteria mentioned in the data processing under item 2.6, a screening of the differential metabolites

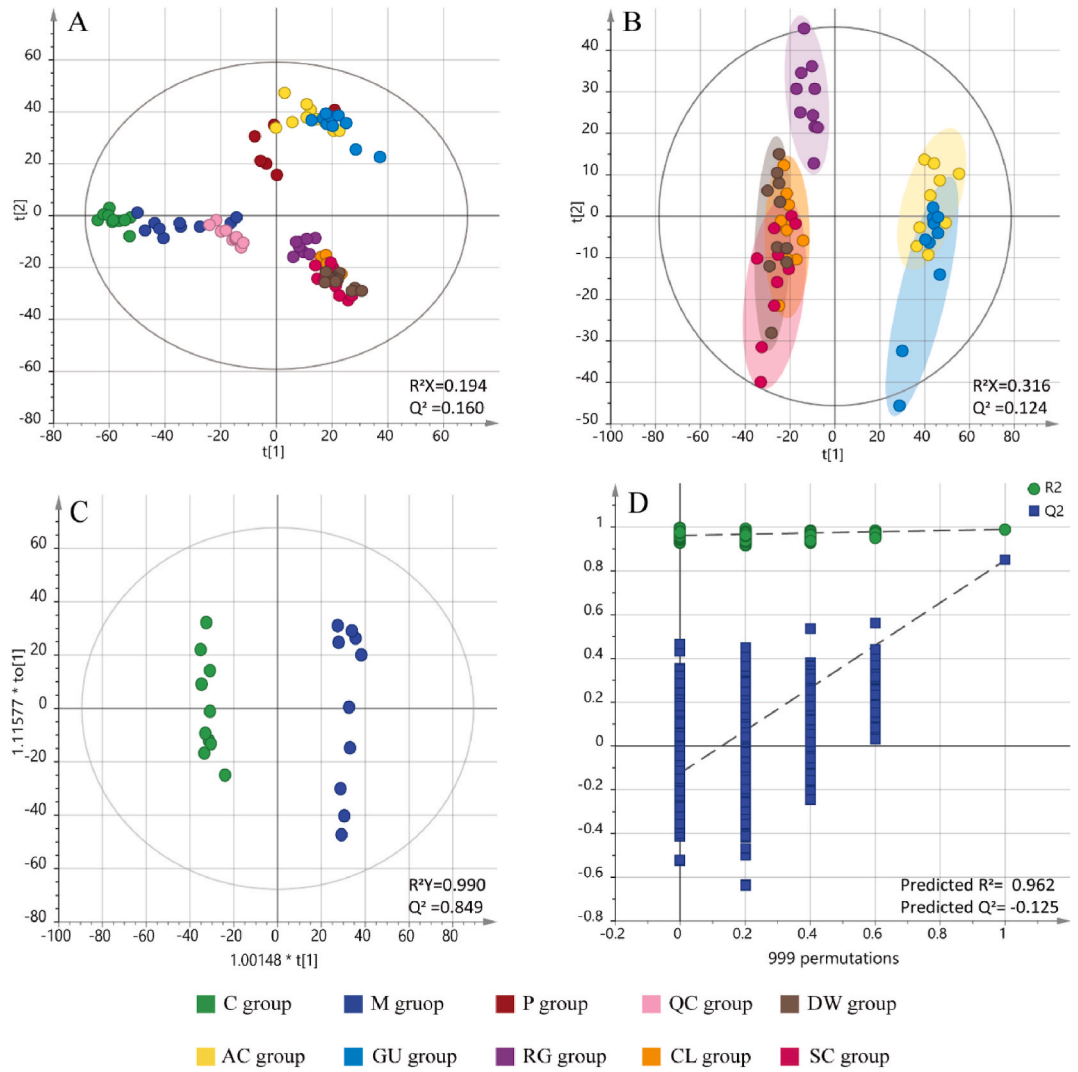

Fig. 2. Multivariate statistical analysis of metabolic profiles from UPLC-QTOF-MS/MS. **A:** PCA score scatter plots obtained from all different groups. **B:** PCA score scatter plots obtained from six TCM treatment groups. **C:** OPLS-DA scores scatter plot of the control and model group. **D:** Plots for 999-time permutation validation test for OPLS-DA models corresponded to the control and model group.

between the control and model groups was conducted (VIP>1, $P < 0.05$ or FC $\geq 1.1/\leq 0.9$). Ultimately, a total of 23 variables were successfully identified as potential biomarkers, and their associated identification information is presented in Table 2. The discriminating metabolites were generally distributed as amino acids, fatty acids, hormones, carnitines and phospholipids. Besides, a comparison of these metabolite's levels between the TCM intervention and model groups was carried out to explore the contribution of each drug in the total prescription. The corresponding variation trends for each metabolite in the different groups were given in Table 3. A detailed list of differentially biomarkers, along with their corresponding fold change values, was shown in Table S2. To further uncover the variable tendencies of the 23 differential metabolites among different groups, a heatmap was employed according to the relative contents of metabolites using GraphPad Prism 9.0. As depicted in Fig. 3, compared with group C, the levels of 11 differential metabolites were up-regulated in the model group, while the levels of 12 differential metabolites were down-regulated than those in control mice. Each intervention exhibited different degrees of NAFLD prevention and treatment effect group by modulating distinct potential biomarkers. AC, CL, SC, RG, and GU groups could regulate 8, 16, 18, 11 and 9 differential metabolites, respectively. A total of 19 differential metabolites were regulated by DWYG prescription, which was confirmed that more than 80 % of the biomarkers in model mice returned to normal levels.

3.3. *Metabolic pathway analysis*

To gain insights into understand the metabolic processes of the metabolites, a pathway analysis was conducted according to the discriminating metabolites listed in Table 2. As shown in Fig. 4, six metabolic pathways involved in the disturbance of NAFLD as

Table 2
UHPLC-QTOF-MS/MS identification of potential biomarkers in mice serum and their related information.

No.	RT (min)	Metabolites	Molecular Formula	Adduct ion	Adduct mass	Actual mass	Error	Fragment ion
1	3.75	Valerylcarnitine	$C_{12}H_{23}NO_4$	$[M+H]^+$	246.1703	246.1705	−0.81	187.10,85.03,57.03
2	6.13	N-Acetyldopamine	$C_{10}H_{13}NO_3$	$[M+H]^+$	196.0952	196.0974	−11.22	152.07,135.04,113.06,107.04
3	11.79	N-Palmitoyl Arginine	$C_{21}H_{34}O_6S$	$[M+H]^+$	415.2116	415.2154	−9.15	155.09,139.15,139.11,116.07
4	15.02	Sphingosine	$C_{18}H_{37}NO_2$	$[M+Na]^+$	322.2720	322.2722	−0.62	264.27,221.23,196.16,137.13
5	15.13	Arachidonoylcarnitine	$C_{27}H_{45}NO_4$	$[M+Na]^+$	448.3420	448.3427	−1.56	448.34,85.03,57.03
6	15.13	6-Methylene-4-pregnene-3,20-dione	$C_{22}H_{30}O_2$	$[M+H]^+$	349.2121	349.2143	−6.30	267.17,239.14,175.11,105.07
7	15.88	LysoPA(22:6)	$C_{25}H_{39}O_7P$	$[M+Na]^+$	505.2309	505.2331	−4.35	311.24,311.24,155.01
8	16.13	LysoPC(22:5)	$C_{30}H_{52}NO_7P$	$[M+Na]^+$	592.3368	592.3379	−1.86	473.26,387.29,184.07,104.11
9	16.23	LysoPC(20:3)	$C_{28}H_{52}NO_7P$	$[M+H]^+$	546.3551	546.356	−1.65	363.29,258.11,240.10,184.07,104.11
10	16.31	PG(TXB2/i-24:0)	$C_{50}H_{93}O_{14}P$	$[M-H]^-$	947.6151	947.6225	−7.81	367.36,171.01,152.99
11	16.33	LysoPE(16:0)	$C_{21}H_{44}NO_7P$	$[M+H]^+$	454.2917	454.2934	−3.74	313.27,257.25,239.24,109.10
12	16.36	MG(22:6/0:0/0:0)	$C_{25}H_{38}O_4$	$[M+Na]^+$	425.2665	425.2668	−0.71	385.27,329.25,269.23,157.10,131.09
13	16.46	MG(18:2/0:0/0:0)	$C_{21}H_{38}O_4$	$[M+Na]^+$	377.2678	377.2668	2.65	337.27,263.24,139.11,121.10
14	16.68	PC(20:5-3OH/2:0)	$C_{30}H_{50}NO_{11}P$	$[M+H]^+$	632.3256	632.3200	8.86	184.07,147.00,125.00,104.11
15	16.68	LysoPC(20:2)	$C_{28}H_{54}NO_7P$	$[M+H]^+$	548.3707	548.3716	−1.64	467.25,365.31,146.98,104.11
16	16.69	5beta-Pregnane-3,20-dione	$C_{21}H_{32}O_2$	$[M+H]^+$	317.2452	317.2481	−9.14	275.24,203.14,193.16,179.14,107.09
17	16.76	PA(20:4-2OH/i-14:0)	$C_{37}H_{65}O_{10}P$	$[M+Na]^+$	723.4340	723.4213	17.56	602.45,495.21,405.2045,387.19
18	17.06	LysoPE(18:0)	$C_{23}H_{48}NO_7P$	$[M+H]^+$	482.3231	482.3247	−3.32	421.17,339.29,285.28,111.12
19	17.65	LysoPI(20:4)	$C_{29}H_{49}O_{12}P$	$[M+Na]^+$	643.2902	643.2859	6.68	361.27,301.07,259.24,147.07
20	18.07	Calcium octadecanoate	$C_{36}H_{70}CaO_4$	$[M+Na]^+$	629.4786	629.4798	−1.91	263.24,123.12,109.10
21	18.22	Ethyl octadec-9-enoate	$C_{20}H_{38}O_2$	$[M+H]^+$	311.2978	311.2950	8.99	265.25,247.24,135.12
22	18.22	dihydrocorticosterone	$C_{21}H_{32}O_4$	$[M+H]^+$	349.2416	349.2379	10.59	271.21,175.11,145.10,125.10
23	18.85	Cerd(18:0/18:0)	$C_{36}H_{73}NO_3$	$[M+H]^+$	568.5667	568.5669	−0.35	550.56,302.31,284.29

Table 3
The 23 identified biomarkers of NAFLD mice treated by DWYG and its single herb with their related information.

No.	Metabolites[a]	VIP[b]	Trend[c]							Metabolic pathways[d]
			M/C	AC/M	CL/M	SC/M	RG/M	GC/M	DW/M	
1	Valerylcarnitine	1.230	↑	–	–	–	–	↓	↓	Fatty acid beta-oxidation
2	N-Acetyldopamine	1.365	↑	↓	↓	↓	↓	↓	↓	Amino acid metabolism
3	N-Palmitoyl Arginine	1.309	↑**	↓	–	–	–	–	↓	Amino acid metabolism
4	Sphingosine	1.361	↑*	–	–	↓	↓	–	↓	Sphingolipid signaling pathway
5	Arachidonoylcarnitine	1.178	↑**	↓	–	–	–	–	–	Fatty acid beta-oxidation
6	6-Methylene-4-pregnene-3,20-dione	1.099	↓	↑	↑	–	↑	↑	–	Steroid hormone biosynthesis
7	LysoPA (22:6)	1.050	↓	–	↑**	↑**	↑**	↑	↑**	Glycerophospholipid metabolism
8	LysoPC (22:5)	1.578	↓**	–	↑*	↑**	↑**	↑**	↑**	Glycerophospholipid metabolism
9	LysoPC (20:3)	1.649	↑**	↓	–	↓**	–	↓**	–	Glycerophospholipid metabolism
10	PG (TXB2/i-24:0)	1.818	↓*	–	↑	↑	–	–	↑	Glycerophospholipid metabolism
11	LysoPE (16:0)	1.741	↓**	–	↑**	↑**	↑*	–	↑**	Glycerophospholipid metabolism
12	MG (22:6/0:0/0:0)	1.869	↓**	–	↑	↑**	↑*	–	↑**	Glycerophospholipid metabolism
13	MG (18:2/0:0/0:0)	2.073	↓**	–	↑	↑**	↑*	–	↑**	Glycerophospholipid metabolism
14	PC (20:5-3OH/2:0)	1.881	↑**	↓**	↓**	↓**	–	↓**	↓*	Glycerophospholipid metabolism
15	LysoPC (20:2)	1.690	↑**	↓**	↓**	↓**	–	↓**	↓**	Glycerophospholipid metabolism
16	5beta-Pregnane-3,20-dione	1.111	↓**	–	–	–	↑	–	–	Steroid hormone biosynthesis
17	PA (20:4-2OH/i-14:0)	1.508	↓**	↓**	↓**	↓**	↓**	↓**	↓**	Glycerophospholipid metabolism
18	LysoPE (18:0)	1.748	↓	–	↑	↑	–	–	↑	Glycerophospholipid metabolism
19	LysoPI (20:4)	1.395	↑**	–	↓**	↓	–	–	↓	Glycerophospholipid metabolism
20	Calcium octadecanoate	1.074	↑*	–	↓**	↓	–	–	↓*	Biosynthesis of unsaturated fatty acids
21	Ethyl octadec-9-enoate	1.688	↓*	–	–	↑	–	–	↑	Biosynthesis of unsaturated fatty acids
22	dihydrocorticosterone	1.302	↓	–	↑	↑	↑*	–	↑	Steroid hormone biosynthesis
23	Cerd (18:0/18:0)	1.256	↑**	–	↓**	↓*	–	–	↓**	Sphingolipid signaling pathway

*$P < 0.05$, **$P < 0.01$, significantly different from model group.

[a] Metabolite identification was carried out by comparison to the METLIN and HMDB Metabolite Databases.

[b] Calculated using the OPLS-DA model based on metabolites of control group and model group of serum samples; Selection was based on VIP values (threshold >1).

[c] Up arrows indicate metabolites were upregulated, and down arrows indicate metabolites were downregulated; Selected metabolites based on FC $\geq$ 1.1 or FC $\leq$ 0.9.

[d] Related pathway was referred to KEGG.

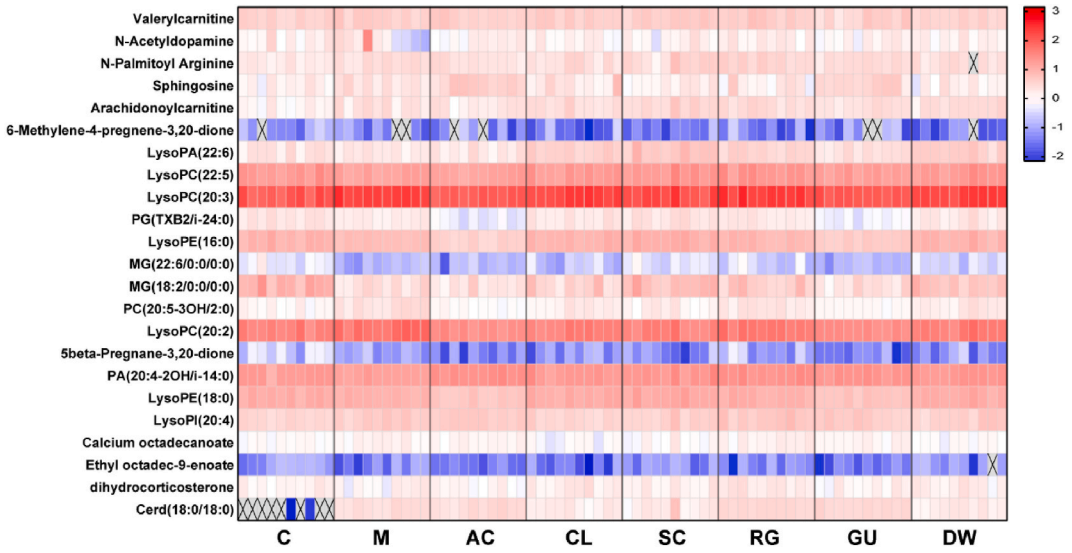

Fig. 3. Distribution of the 23 biomarkers in the serum samples from different groups. Values at each color block was the ratio of the peak area of a metabolite to that of the internal standard after the log10 transformation. A blue color indicated down-regulation of metabolites while a red color indicated up-regulation of metabolites. The grey squares with a cross on the heat map indicated that the metabolites were not detected in the sample.

follows: (1) Steroid hormone biosynthesis; (2) Glycerophospholipid metabolism; (3) Sphingolipid signaling pathway; (4) Fatty acid beta-oxidation; (5) Biosynthesis of unsaturated fatty acids; (6) Amino acid metabolism. In addition, the most relevant pathways regulated by AC were (2) Glycerophospholipid metabolism and (6) Amino acid metabolism. The most relevant pathway regulated by

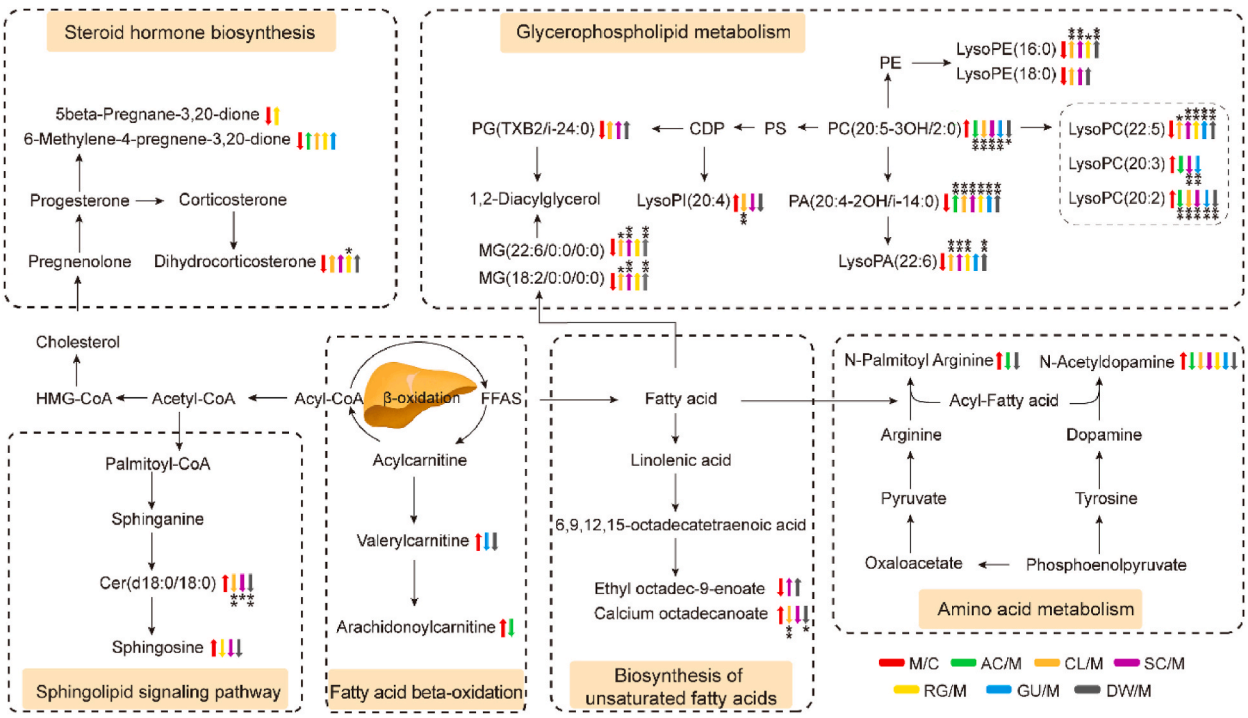

Fig. 4. Metabolic pathway networks involved in the treatment of DWYG on HFD-induced NAFLD. The variation trend of metabolites in model group compared with control group is indicated as red arrows, while green, orange, purple, yellow, blue and dark grey arrows represent the regulatory trend in AC, CL, SC, RG, GU and DW groups relative to model group, respectively. Up arrows indicate that the trend of the change of metabolites is rising, and down arrows indicate that the trend of the change of metabolites is declining. $^{*}P < 0.05$, $^{**}P < 0.01$, significantly different from model group.

CL was (2) Glycerophospholipid metabolism. The most relevant pathways regulated by SC were (2) Glycerophospholipid metabolism, (3) Sphingolipid signaling pathway and (5) Biosynthesis of unsaturated fatty acids. The most relevant pathways regulated by RG were (2) Glycerophospholipid metabolism, (3) Sphingolipid signaling pathway and (5) Biosynthesis of unsaturated fatty acids. The most relevant pathways regulated by GU were (2) Glycerophospholipid metabolism and (4) Fatty acid beta-oxidation. Among them, glycerophospholipid metabolism pathway was modulated by all TCM intervention groups, indicating that synergistic effects of DWYG preparation were responsible for regulating this pathway. In addition, all six pathways disturbed in the mice of the model group were found to be involved in the hepatoprotective effects of DWYG on mice with high fat diets.

3.4. Combined mechanism of DWYG on NAFLD

To improve the visualization, the overall metabolic intervention mechanism of the combined application of DWYG for nonalcoholic fatty liver disease was displayed as a network. As shown in Fig. 5, the metabolic pathways related to anti-NAFLD of DWYG formula included the primary metabolic pathways of each single drug, manifesting that the prevention and therapeutic effect of DWYG prescription for NAFLD was comprehensive. In this network, the degree values of SC, CL and DWYG were 18, 16 and 19 respectively, which indicated that the ability of SC and CL to reverse abnormal metabolism was only second to that of DWYG. Thus, among the five herbs of DWYG formula, SC and CL exhibited the highest degree of correlation in terms of their ability to regulate disordered metabolism in NAFLD mice.

4. Discussion

In this study, we explored the protective effects and potential combined mechanism of action of DWYG on NAFLD induced by HFD diets for the first time from the perspective of untargeted metabolomics and disassembled prescriptions. The results showed that DWYG formula possessed more pronounced hypolipidemic effect compared to a single herb, as evidenced by serum biochemistry and pathological observations in NAFLD mice. For another, DWYG formula and each individual herb had different regulatory mechanisms. DWYG has been found to exhibit a greater capacity for regulating metabolites and metabolic pathways than AC, CL, SC, RG or GU respectively, mainly involving lipid metabolism. In addition, SC and CL could be the key herbs that were involved in treating NAFLD by DWYG.

It was worth noting that the regulation of glycerophospholipid metabolism was present in all TCM intervention groups in the present study. This finding indicated that glycerophospholipid metabolism was modulated by multiple constituents via multiple targets, which might be due to the synergism of complete composition in five herbs of DWYG. The great changeable LysoPC(20:2), LysoPC(20:3) and LysoPC(22:5) in the model group, observed in this study, were polyunsaturated LysoPCs, in line with a previous report that dysregulated LysoPC levels were involved in diet induced NAFLD in mice [30]. The biological function of LysoPCs depends on the Acyl length and the saturation degree of fatty acids and is influenced by endogenous synthesis and diet [31,32]. Moreover, many LysoPC species were reported to be increased in NAFLD that were closely related to pro-inflammatory activity and oxidative stress [33–35]. By the action of lysophopholipaseD, LysoPCs were quickly converted into LysoPA and PA [36]. We found that PA and LysoPA,

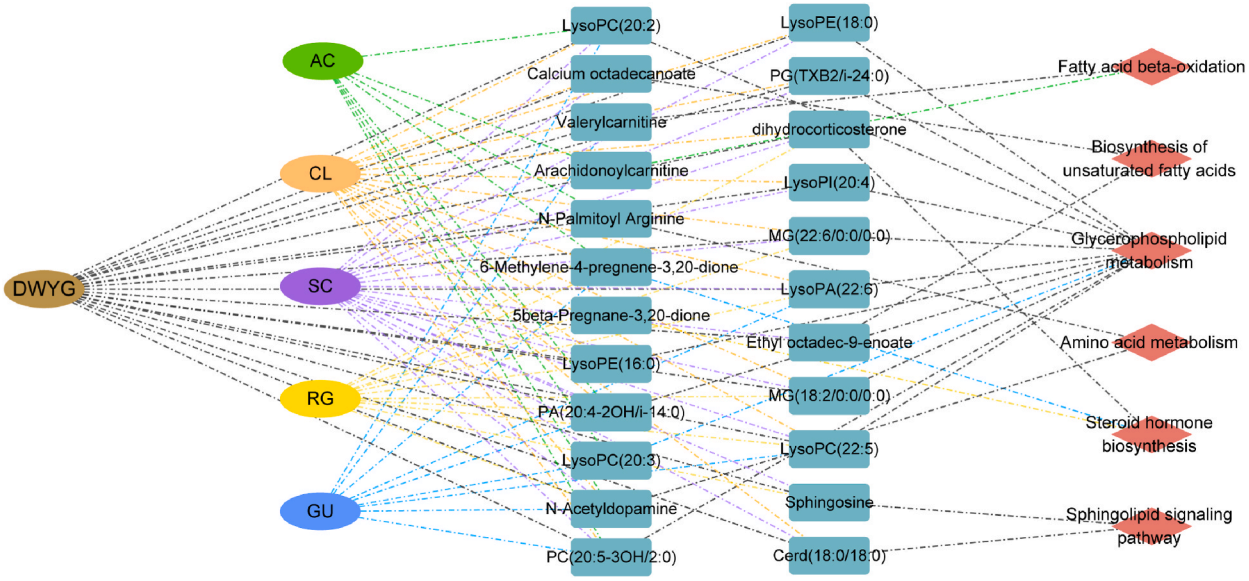

Fig. 5. Network analysis of the synergistic mechanism of DWYG for preventing and treating NAFLD. The pieces connected with the black lines represent related biomarkers and metabolic pathways regulated by DWYG prescription on NAFLD. The pieces connected with the green, orange, purple, yellow and blue lines represent related biomarkers and metabolic pathways regulated by AC, CL, SC, RG, and GU on NAFLD, respectively.

which were lipid second messenger, were as well as governor regulator of inflammation [37,38], significantly associated with NAFLD. LysoPE has also been reported to have an effect on the reduction of liver inflammation and the normalization of serum biomarkers in mice with liver disease [39]. On the basis of the metabolite data, it was observed that DWYG modified the levels of lysophospholipids and phospholipids, indicating that DWYG might be the underlying metabolic mechanism responsible for its effect on NAFLD by protecting against inflammation.

We also found that sphingosine and cer(d18:0/18:0), which were involved in the sphingolipid metabolism pathway, were inhibited by DWYG and RG in NAFLD mice. Ceramide was a lipotoxic factor, which played an important role in apoptosis and stress response. Inhibiting ceramide production might delay or prevent disease development [40]. Sphingosine, one of the most biologically active sphingolipids, was significantly increased in NAFLD mice in this study, which was corresponded with previous research. It was reported that sphingosine could reduce insulin sensitivity and accelerate hepatic steatosis in obese rodents [41]. As reported, the disorganization of sphingolipid signaling pathway was contacted with inflammatory signaling [42] and cellular immunity response [43,44] in many chronic metabolic diseases, such as obesity, type 2 diabetes mellitus and NAFLD. In addition, studies found that RG had an enhancement of immune function [45]. As a consequence, it was reasonable to speculate that RG in DWYG contributed to resisting disturbances in the sphingolipid signaling pathway caused by external stimuli through continuously activating the immune system.

Furthermore, our study discovered that the fatty acid beta-oxidation acts as a bridge among other disordered metabolic pathways. Of paramount characteristics for NAFLD are its ineffective capacity to fatty acid oxidation in mitochondria and its augmented hepatic fatty acid synthesis [46]. What's more, increased long-chain acylcarnitines (AC) and short-chain ACs are likely to be important in increasing mitochondrial lipolysis as well as fatty acid oxidation, respectively [47]. This indicates that the increase in serum AC after HFD feeding is due to the increased hepatic uptake and utilization of fatty acids in HFD. Therefore, DWYG and GU might firsthand protect the liver by inhibiting acylcarnitine elevation of fatty acid beta-oxidation.

In addition, fatty acid beta-oxidation has been shown to be involved in the modulation of steroid hormones at multiple levels, thereby affecting hepatic steatosis [48]. Increasing data showed that a significant role was played by sex hormones in the pathological progression of NAFLD [48]. In this study, the concentrations of several gonadal hormones, such as dihydrocorticosterone, 5beta-Pregnane-3,20-dione and 6-Methylene-4-pregnene-3,20-dione, were significantly decreased in NAFLD mice, while RG could reverse their abnormal descent after four weeks' treatment. In the absence of estrogen, there might be a higher tendency for increasing in visceral tissue fat and promoting systemic insulin resistance [49]. Male patients with androgen deficiency, such as testosterone, exhibited high prevalence of NAFLD, which was mainly due to the fact that androgens could promote de novo lipid synthesis and inhibit fatty acid oxidation activity [50,51]. Many sex hormones derived from pregnenolone and primarily metabolized in the liver, including estrogen, progesterone, and testosterone [52]. Therefore, we concluded that RG might regulate the pregnenolone level, and further sustain steroid hormone balance, which was in accordance with another study showing RG could restore metabolic disorders via modulating steroid hormone biosynthesis [53].

As for amino acid metabolism regulated by DWYG, it was reported that an elevated serum amino acid level might indicate obesity-associated NAFLD, and mitochondrial dysfunction could impair amino acids metabolism [54]. And amino acid metabolism in NAFLD was strongly related to insulin resistance [55]. There was evidence that consumption of a high-cholesterol diet resulted in an increase in most amino acids and polyamines [56], which was consistent with our results. Our results of NAFLD mice treated with DWYG, showed a reduction of N-Palmitoyl Arginine and N-Acetyldopamine, suggesting that DWYG could inhibit the development of insulin resistance and mitochondrial dysfunction by improving the disorder of amino acid metabolism.

With regard to the number of potential biomarkers and metabolic pathways regulated by DWYG during the treatment of NAFLD, DWYG exhibited the most comprehensive anti-NAFLD effects. Numerous studies have shown that the irreplaceable advantages of synergistic effects in herbal therapies were manifested when multiple herbal extracts were used, resulting in better efficacy compared to individual herbs in TCM prescriptions [7,22]. The therapeutic effect of TCM prescriptions was not only related to the efficacy of each part comprised in the formula but also to the interaction between the constituent herbs [7]. DWYG is a holistic formula that contains five Chinese herbal medicines, so that the combination of these efficacy groups and the synergistic interactions between multiple ingredients may contribute to the overall therapeutic actions of DWYG. In addition, our results indicated that CL and SC play an essential role in the modulation of potential biomarkers in the absence of the DWYG functional unit. It was approximately consistent with the tendency in PCA score plots, which manifested as CL and SC groups had a considerable overlap with DWYG group, illustrating that the function of the TCM intervention could be reflected in the selection of potential biomarkers. In this study, 16 and 18 perturbed metabolites were regulated after administering CL and SC, respectively, which corresponded to CL correct abnormalities in glycerophospholipid metabolism and SC correct abnormalities in sphingolipid signaling pathway, biosynthesis of unsaturated fatty acids and glycerophospholipid metabolism. It has been reported that *Curcuma longa* L. extract and its main active ingredient curcumin counteract hepatic dyslipidemia via the regulation of ER stress [14] and *Curcuma longa* L. extract had powerful effects on affecting glycerophospholipid metabolism might be involved in the prevention of NAFLD [57]. SC had inhibition of liver cell apoptosis and promotion of liver regeneration effects [58] and has been shown to reduce lipid accumulation in the liver [59] and regulate glycerophospholipid metabolism [60] to protect the liver.

5. Conclusion

In the current study, an integrated strategy combining disassembled prescriptions and untargeted metabolomic has been established to systematically clarify the combined intervention mechanism of DWYG in NAFLD. As a result, a total of 23 potential biomarkers have been found, and 19 metabolites could be regulated by DWYG among them. The mechanism of DWYG prescription

reduced the HFD-induced disorders of liver function, which were related to steroid hormone biosynthesis, glycerophospholipid metabolism, sphingolipid signaling pathway, fatty acid beta-oxidation, biosynthesis of unsaturated fatty acids, and amino acid metabolism. Compared with its five single groups, DWYG had the strongest anti-NAFLD effect and the most extensive metabolic regulation. Among them, CL and SC played a key role in treating NAFLD. This study will provide a reference for the clinical application of DWYG and avail further understanding of the synergistic mechanism of DWYG prescriptions.

Ethics statement

This study was reviewed and approved by the Institutional Animal Care and Use Committee of Hubei University of Chinese Medicine, with the approval number: 202203004.

Data availability statement

Data will be made available on request.

Funding statement

This work was supported by the project of Hubei Provincial Administration of Traditional Chinese Medicine [grant number ZY2023Q040].

CRediT authorship contribution statement

Jinlin Xu: Writing – original draft, Methodology, Data curation. **Yuehui Jin:** Writing – original draft, Methodology, Data curation. **Chengwu Song:** Supervision, Project administration, Conceptualization. **Guangya Chen:** Visualization, Investigation. **Qiaoyu Li:** Investigation. **Hao Yuan:** Investigation. **Sha Wei:** Methodology, Formal analysis. **Min Yang:** Methodology, Formal analysis. **Sen Li:** Writing – review & editing, Supervision. **Shuna Jin:** Writing – review & editing, Supervision, Project administration.

Declaration of competing interest

The authors declare that they have no known competing financial interests or personal relationships that could have appeared to influence the work reported in this paper.

Appendix A. Supplementary data

Supplementary data to this article can be found online at https://doi.org/10.1016/j.heliyon.2023.e22151.

References

[1] M. Masarone, J. Troisi, A. Aglitti, P. Torre, A. Colucci, M. Dallio, A. Federico, C. Balsano, M. Persico, Untargeted metabolomics as a diagnostic tool in NAFLD: discrimination of steatosis, steatohepatitis and cirrhosis, Metabolomics 17 (2) (2021) 1–13, https://doi.org/10.1007/s11306-020-01756-1.

[2] M.S. Mundi, S. Velapati, J. Patel, T.A. Kellogg, B.K. Abu Dayyeh, R.T. Hurt, Evolution of NAFLD and its management, Nutr. Clin. Pract. 35 (1) (2020) 72–84, https://doi.org/10.1002/ncp.10449.

[3] F. Ren, Q.P. Chen, C. Meng, H.M. Chen, Y.J. Zhou, H. Zhang, W.J. Chen, Serum metabonomics revealed the mechanism of Ganoderma amboinense polysaccharides in preventing non-alcoholic fatty liver disease (NAFLD) induced by high-fat diet, J. Funct.Foods 82 (2021), 104496, https://doi.org/10.1016/j.jff.2021.104496.

[4] A.R. Araujo, N. Rosso, G. Bedogni, C. Tiribelli, S. Bellentani, Global epidemiology of non-alcoholic fatty liver disease/non-alcoholic steatohepatitis: what we need in the future, Liver Int. 38 (2018) 47–51, https://doi.org/10.1111/liv.13643.

[5] P. Mehta, S. Lohidasan, K. Mahadik, Pharmacokinetic behaviour of clinically important TCM prescriptions, Orient, Pharm. Exp. Med. 17 (3) (2017) 171–188, https://doi.org/10.1007/s13596-017-0281-y.

[6] J. Shen, Z.J. Pu, J. Kai, A. Kang, Y.P. Tang, L.L. Shang, G.S. Zhou, Z.H. Zhu, E.X. Shang, S.P. Li, Y.J. Cao, W.W. Tao, S.L. Su, L. Zhang, H. Zhou, D.W. Qian, J. A. Duan, Comparative metabolomics analysis for the compatibility and incompatibility of kansui and licorice with different ratios by UHPLC-QTOF/MS and multivariate data analysis, J. Chromatogr., B: Anal. Technol. Biomed. Life Sci. 1057 (2017) 40–45, https://doi.org/10.1016/j.jchromb.2017.04.042.

[7] X. Zhou, S.W. Seto, D. Chang, H. Kiat, V. Razmovski-Naumovski, K. Chan, A. Bensoussan, Synergistic effects of Chinese herbal medicine: a comprehensive review of methodology and current research, Front. Pharmacol. 7 (2016) 201, https://doi.org/10.3389/fphar.2016.00201.

[8] Z.H. Ye, X. Gao, B.B. Zhao, H.M. Li, M. Wan, N. Wu, M.X. Chang, S.S. Cheng, Diwu Yanggan capsule inhibits the occurrence and development of liver cancer in the Solt-Farber rat model by regulating the Ras/Raf/Mek/Erk signaling pathway, Am. J. Transl. Res. 10 (11) (2018) 3797–3805. https://pubmed.ncbi.nlm.nih.gov/30662630.

[9] B.B. Zhao, Z.H. Ye, X. Gao, H.M. Li, Diwu yanggan modulates the wnt/beta-catenin pathway and inhibits liver carcinogenesis signaling in 2-AAF/PH model rats, Curr. Med. Sci. 39 (6) (2019) 913–919, https://doi.org/10.1007/s11596-019-2123-2.

[10] H.M. Li, Z.H. Ye, X. Gao, L.S. Zhang, X. Yao, J.X. Gu, D.B. Lu, M. Wan, L. Xiao, W.X. Cai, X.S. Yan, B.B. Zhao, Y. Wu, J.R. Zhang, Diwu Yanggan capsule improving liver histological response for patients with HBeAg-negative chronic hepatitis B: a randomized controlled clinical trial, Am. J. Transl. Res. 10 (5) (2018) 1511–1521. https://pubmed.ncbi.nlm.nih.gov/29887964.

[11] X. Shen, S.S. Cheng, Y. Peng, H.L. Song, H.M. Li, Attenuation of early liver fibrosis by herbal compound "Diwu Yanggan" through modulating the balance between epithelial-to-mesenchymal transition and mesenchymal-to-epithelial transition, BMC Complem. Altern. Med. 14 (2014) 418, https://doi.org/10.1186/1472-6882-14-418.

[12] J.L. Xu, F. Zou, Y.Q. Lin, Z.X. Zeng, Y.K. Liu, L.J. Zhang, R.Z. Huang, X.G. Li, C.W. Song, Y.P. Tang, S.N. Jin, Integrated serum metabolomics and network pharmacology approach to reveal the potential mechanisms of diwuyanggan prescription in the prevention of acute liver injury, Nat. Prod. Commun. 18 (6) (2023), https://doi.org/10.1177/1934578X231180076.
[13] S.H. Hong, S.H. Seo, J.H. Lee, B.T. Choi, The aqueous extract from Artemisia capillaris Thunb. inhibits lipopolysaccharide-induced inflammatory response through preventing NF-κB activation in human hepatoma cell line and rat liver, Int. J. Mol. Med. 13 (5) (2004) 717–720, https://doi.org/10.3892/ijmm.13.5.717.
[14] H.Y. Lee, S.W. Kim, G.H. Lee, M.K. Choi, H.W. Chung, Y.C. Lee, H.R. Kim, H.J. Kwon, H.J. Chae, Curcumin and Curcuma longa L. extract ameliorate lipid accumulation through the regulation of the endoplasmic reticulum redox and ER stress, Sci. Rep. 7 (1) (2017) 1–14, https://doi.org/10.1038/s41598-017-06872-y.
[15] Y.O. Song, S.J. Lee, H.J. Park, S.H. Jang, B.Y. Chung, Y.M. Song, G.S. Kim, J.H. Cho, Hepatoprotective effect of Schisandra chinensis on high-fat diet-induced fatty liver in rats, Korean J. Vet. Res. 36 (1) (2013) 45–52, https://doi.org/10.7853/kjvs.2013.36.1.45.
[16] R.J. Zhang, Y. Zhao, Y.F. Sun, X.S. Lu, X.B. Yang, Isolation, characterization, and hepatoprotective effects of the raffinose family oligosaccharides from Rehmannia glutinosa Libosch, J. Agric. Food Chem. 61 (32) (2013) 7786–7793, https://doi.org/10.1021/jf4018492.
[17] J.L. Du, R. Jia, L.P. Cao, Z.Y. Gu, Q. He, P. Xu, G.J. Yin, Y.Z. Ma, Regulatory effects of Glycyrrhiza total flavones on fatty liver injury induced by a high-fat diet in tilapia (Oreochromis niloticus) via the Nrf2 and TLR signaling pathways, Aquacult. Int. 30 (2022) 1527–1548, https://doi.org/10.1007/s10499-021-00787-2.
[18] Y.Y. Liu, M.Y. Wei, K.X. Yue, R.J. Wang, Y.H. Ma, L.H. Men, Z.F. Pi, Z.Q. Liu, Z.Y. Liu, Non-target metabonomic method provided new insights on the therapeutical mechanism of Gancao Fuzi decoction on rheumatoid arthritis rats, J. Chromatogr., B: Anal. Technol. Biomed. Life Sci. 1105 (2019) 93–103, https://doi.org/10.1016/j.jchromb.2018.11.015.
[19] D.N. Cui, X. Wang, J.Q. Chen, B. Lv, P. Zhang, W. Zhang, Z.J. Zhang, F.G. Xu, Quantitative evaluation of the compatibility effects of huangqin decoction on the treatment of irinotecan-induced gastrointestinal toxicity using untargeted metabolomics, Front. Pharmacol. 8 (2017) 211, https://doi.org/10.3389/fphar.2017.00211.
[20] L.J. Wang, X.B. Jia, Y. Chen, L. Feng, S.H. Song, Thoughts and methods of research on Chinese medicine compound prescription, Chin. Tradit. Pat. Med. (9) (2008) 1343–1346, https://doi.org/10.3969/j.issn.1001-1528.2008.09.031.
[21] R. Ma, Q. Xie, J. Wang, L.H. Huang, X.Q. Guo, Y.M. Fan, Combination of urine and faeces metabolomics to reveal the intervention mechanism of Polygala tenuifolia compatibility with Magnolia officinalis on gastrointestinal motility disorders, J. Pharm. Pharmacol. 73 (2) (2021) 247–262, https://doi.org/10.1093/jpp/rgaa022.
[22] J.X. Wu, H. Zheng, X. Yao, X.W. Liu, H.J. Zhu, C.L. Yin, X. Liu, Y.Y. Mo, H.M. Huang, B. Cheng, F. Wu, Z.N. Chen, F.M. Song, J.X. Ruan, H.Y. Zhang, P. Liu, Y. H. Liang, H. Song, H.W. Guo, Z.H. Su, Comparative analysis of the compatibility effects of Danggui-Sini Decoction on a blood stasis syndrome rat model using untargeted metabolomics, J. Chromatogr., B: Anal. Technol. Biomed. Life Sci. 1105 (2019) 164–175, https://doi.org/10.1016/j.jchromb.2018.12.017.
[23] J.K. Nicholson, J.C. Lindon, Systems biology: metabonomics, Nature 455 (7216) (2008) 1054–1056, https://doi.org/10.1038/4551054a.
[24] X.J. Liu, M. Lv, Y.Z. Wang, D. Zhao, S.J. Zhao, S.Y. Li, X.M. Qin, Deciphering the compatibility rules of traditional Chinese medicine prescriptions based on NMR metabolomics: a case study of Xiaoyaosan, J. Ethnopharmacol. 254 (2020), 112726, https://doi.org/10.1016/j.jep.2020.112726.
[25] M. Wang, L. Chen, D. Liu, H. Chen, D.D. Tang, Y.Y. Zhao, Metabolomics highlights pharmacological bioactivity and biochemical mechanism of traditional Chinese medicine, Chem. Biol. Interact. 273 (2017) 133–141, https://doi.org/10.1016/j.cbi.2017.06.011.
[26] X.L. Xiang, C. Su, Q.X. Shi, J.N. Wu, Z.X. Zeng, L.J. Zhang, S.N. Jin, R.Z. Huang, T.X. Gao, C.W. Song, Potential hypoglycemic metabolites in dark tea fermented by Eurotium cristatum based on UPLC-QTOF-MS/MS combining global metabolomic and spectrum-effect relationship analyses, Food Funct. 12 (16) (2021) 7546–7556, https://doi.org/10.1039/D1FO00836F.
[27] M.X. Dai, S. Li, Q.X. Shi, X.L. Xiang, Y.H. Jin, S. Wei, L.J. Zhang, M. Yang, C.W. Song, R.Z. Huang, S.N. Jin, Changes in triterpenes in alismatis rhizoma after processing based on targeted metabolomics using UHPLC-QTOF-MS/MS, Molecules 27 (1) (2021) 185, https://doi.org/10.3390/molecules27010185.
[28] C.W. Song, Q.S. Yu, X.H. Li, S.N. Jin, S. Li, Y. Zhang, S.L. Jia, C. Chen, Y. Xiang, H.L. Jiang, The hypolipidemic effect of total saponins from kuding tea in high-fat diet-induced hyperlipidemic mice and its composition characterized by UPLC-QTOF-MS/MS, J. Food Sci. 81 (5) (2016) H1313–H1319, https://doi.org/10.1111/1750-3841.13299.
[29] J. Jansson, B. Willing, M. Lucio, A. Fekete, J. Dicksved, J. Halfvarson, C. Tysk, P. Schmitt-Kopplin, Metabolomics reveals metabolic biomarkers of Crohn's disease, PLoS One 4 (7) (2009), e6386, https://doi.org/10.1371/journal.pone.0006386.
[30] M.I. Ahmad, M.U. Ijaz, M. Hussain, I.A. Khan, N. Mehmood, S.M. Siddiqi, C.C. Liu, D. Zhao, X.L. Xu, G.Z. Zhou, C.B. Li, High fat diet incorporated with meat proteins changes biomarkers of lipid metabolism, antioxidant activities, and the serum metabolomic profile in Glrx1(-/-) mice, Food Funct. 11 (1) (2020) 236–252, https://doi.org/10.1039/C9FO02207D.
[31] R.C. Block, R. Duff, P. Lawrence, L. Kakinami, J.T. Brenna, G.C. Shearer, N. Meednu, S. Mousa, A. Friedman, W.S. Harris, M. Larson, S. Georas, The effects of EPA, DHA, and aspirin ingestion on plasma lysophospholipids and autotaxin, Prostag. Leukotr. Ess. 82 (2–3) (2010) 87–95, https://doi.org/10.1016/j.plefa.2009.12.005.
[32] S. Akagi, N. Kono, H. Ariyama, H. Shindou, T. Shimizu, H. Arai, Lysophosphatidylcholine acyltransferase 1 protects against cytotoxicity induced by polyunsaturated fatty acids, Faseb. J. 30 (5) (2016) 2027–2039, https://doi.org/10.1096/fj.201500149.
[33] H.J. Kim, J.H. Kim, S. Noh, H.J. Hur, M.J. Sung, J.T. Hwang, J.H. Park, H.J. Yang, M.S. Kim, D.Y. Kwon, S.H. Yoon, Metabolomic analysis of livers and serum from high-fat diet induced obese mice, J. Proteome Res. 10 (1) (2011) 722–731, https://doi.org/10.1021/pr100892r.
[34] L.L. Chen, Y.F. Chao, P.C. Cheng, N. Li, H.N. Zheng, Y.J. Yang, UPLC-QTOF/MS-Based metabolomics reveals the protective mechanism of hydrogen on mice with ischemic stroke, Neurochem. Res. 44 (8) (2019) 1950–1963, https://doi.org/10.1007/s11064-019-02829-x.
[35] N.D. Hung, D.E. Sok, M.R. Kim, Prevention of 1-palmitoyl lysophosphatidylcholine-induced inflammation by polyunsaturated acyl lysophosphatidylcholine, Inflamm. Res. 61 (5) (2012) 473–483, https://doi.org/10.1007/s00011-012-0434-x.
[36] B. Wang, P. Tontonoz, Phospholipid remodeling in physiology and disease, Annu. Rev. Physiol. 81 (2019) 165–188, https://doi.org/10.1146/annurev-physiol-020518-114444.
[37] J.G. Lee, S.H. Lee, D.W. Park, Y.S. Bae, S.S. Yun, J.R. Kim, S.H. Baek, Phosphatidic acid as a regulator of matrix metalloproteinase-9 expression via the TNF-α signaling pathway, Febs Lett 581 (4) (2007) 787–793, https://doi.org/10.1016/j.febslet.2007.01.048.
[38] M. Barzegar, M. Chandra, J. Yun, P. Harriss, S. Abdehou, S. Miryala, M. Boktor, P. Jordan, D. Escalante-Alcalde, M. Panchatcharam, P068 Lipid phosphate phosphatase-3 (LPP3) deficiency intensifies intestinal inflammation in the dss model of ulcerative colitis: roles of lysophosphatidic acid and lymphatic/vascular networks in infammatory gut injury? Gastroenterology 154 (1) (2018) S35–S36, https://doi.org/10.1053/j.gastro.2017.11.106.
[39] L.G. Chen, C.W. Chang, J.G. Tsay, B.B.C. Weng, Hepatoprotective effects of litchi (Litchi chinensis) procyanidin A2 on carbon tetrachloride-induced liver injury in ICR mice, Exp. Ther. Med. 13 (6) (2017) 2839–2847, https://doi.org/10.3892/etm.2017.4358.
[40] B.T. Bikman, S.A. Summers, Ceramides as modulators of cellular and whole-body metabolism, J. Clin. Invest. 121 (11) (2011) 4222–4230, https://doi.org/10.1172/JCI57144.
[41] L.A. Cowart, Sphingolipids: players in the pathology of metabolic disease, Trends Endocrinol. Metab. 20 (1) (2009) 34–42, https://doi.org/10.1016/j.tem.2008.09.004.
[42] M. Maceyka, S. Spiegel, Sphingolipid metabolites in inflammatory disease, Nature 510 (7503) (2014) 58–67, https://doi.org/10.1038/nature13475.
[43] J. Diab, T. Hansen, R. Goll, H. Stenlund, M. Ahnlund, E. Jensen, T. Moritz, J. Florholmen, G. Forsdahl, Lipidomics in ulcerative colitis reveal alteration in mucosal lipid composition associated with the disease state, Inflamm. Bowel Dis. 25 (11) (2019) 1780–1787, https://doi.org/10.1093/ibd/izz098.
[44] R. Monteiro, I. Azevedo, Chronic inflammation in obesity and the metabolic syndrome, Mediat. Inflamm. 2010 (2010), 289645, https://doi.org/10.1155/2010/289645.
[45] Y. Huang, C.M. Jiang, Y.L. Hu, X.J. Zhao, C. Shi, Y. Yu, C. Liu, Y. Tao, H.R. Pan, Y.B. Feng, J.G. Liu, Y. Wu, D.Y. Wang, Immunoenhancement effect of rehmannia glutinosa polysaccharide on lymphocyte proliferation and dendritic cell, Carbohy. Polym. 96 (2) (2013) 516–521, https://doi.org/10.1016/j.carbpol.2013.04.018.

[46] A. Besse-Patin, M. Leveille, D. Oropeza, B.N. Nguyen, A. Prat, J.L. Estall, Estrogen signals through peroxisome proliferator-activated receptor-gamma coactivator 1alpha to reduce oxidative damage associated with diet-induced fatty liver disease, Gastroenterology 152 (1) (2017) 243–256, https://doi.org/10.1053/j.gastro.2016.09.017.
[47] L.F. Iannucci, F. Cioffi, R. Senese, F. Goglia, A. Lanni, P.M. Yen, R.A. Sinha, Metabolomic analysis shows differential hepatic effects of T2 and T3 in rats after short-term feeding with high fat diet, Sci. Rep. 7 (1) (2017) 1–10, https://doi.org/10.1038/s41598-017-02205-1.
[48] M. Yang, F. Ma, M. Guan, Role of steroid hormones in the pathogenesis of nonalcoholic fatty liver disease, Metabolites 11 (5) (2021) 320, https://doi.org/10.3390/metabo11050320.
[49] M.E. Jones, A.W. Thorburn, K.L. Britt, K.N. Hewitt, N.G. Wreford, J. Proietto, O.K. Oz, B.J. Leury, K.M. Robertson, S. Yao, Aromatase-deficient (ArKO) mice have a phenotype of increased adiposity, Proc. Natl. Acad. Sci. 97 (23) (2000) 12735–12740, https://doi.org/10.1073/pnas.97.23.12735.
[50] A. Barbonetti, M.R.C. Vassallo, M. Cotugno, G. Felzani, S. Francavilla, F. Francavilla, Low testosterone and non-alcoholic fatty liver disease: evidence for their independent association in men with chronic spinal cord injury, J. Spinal Cord Med. 39 (4) (2016) 443–449, https://doi.org/10.1179/2045772314Y.0000000288.
[51] H. Phan, A. Richard, M. Lazo, W.G. Nelson, S.R. Denmeade, J. Groopman, N. Kanarek, E.A. Platz, S. Rohrmann, The association of sex steroid hormone concentrations with non-alcoholic fatty liver disease and liver enzymes in US men, Liver Int. 41 (2) (2021) 300–310, https://doi.org/10.1111/liv.14652.
[52] C.E. Marx, D.W. Bradford, R.M. Hamer, J.C. Naylor, T.B. Allen, J.A. Lieberman, J.L. Strauss, J. Kilts, Pregnenolone as a novel therapeutic candidate in schizophrenia: emerging preclinical and clinical evidence, Neuroscience 191 (2011) 78–90, https://doi.org/10.1016/j.neuroscience.2011.06.076.
[53] T.S. Xia, X. Dong, Y.P. Jiang, L.Y. Lin, Z.M. Dong, Y. Shen, H.L. Xin, Q.Y. Zhang, L.P. Qin, Metabolomics profiling reveals rehmanniae radix preparata extract protects against glucocorticoid-induced osteoporosis mainly via intervening steroid hormone biosynthesis, Molecules 24 (2) (2019) 253, https://doi.org/10.3390/molecules24020253.
[54] E.H. van den Berg, J.L. Flores-Guerrero, E.G. Gruppen, M.H. de Borst, J. Wolak-Dinsmore, M.A. Connelly, S.J. Bakker, R.P. Dullaart, Non-alcoholic fatty liver disease and risk of incident type 2 diabetes: role of circulating branched-chain amino acids, Nutrients 11 (3) (2019) 705, https://doi.org/10.3390/nu11030705.
[55] M. Masoodi, A. Gastaldelli, T. Hyötyläinen, E. Arretxe, C. Alonso, M. Gaggini, J. Brosnan, Q.M. Anstee, O. Millet, P. Ortiz, Metabolomics and lipidomics in NAFLD: biomarkers and non-invasive diagnostic tests, Nat. Rev. Gastroenterol. Hepatol. 18 (12) (2021) 835–856, https://doi.org/10.1038/s41575-021-00502-9.
[56] D. González-Peña, D. Dudzik, A. García, B. de Ancos, C. Barbas, C. Sánchez-Moreno, Metabolomic fingerprinting in the comprehensive study of liver changes associated with onion supplementation in hypercholesterolemic Wistar rats, Int. J. Mol. Sci. 18 (2) (2017) 267, https://doi.org/10.3390/ijms18020267.
[57] Y. Wang, M. Niu, R.S. Li, Y.M. Zhang, C.E. Zhang, Y.K. Meng, H.R. Cui, Z.J. Ma, D.H. Li, J.B. Wang, Untargeted metabolomics reveals intervention effects of total turmeric extract in a rat model of nonalcoholic fatty liver disease, Evid. Based Complement. Alternat. Med. (2016), 8495953, https://doi.org/10.1155/2016/8495953, 2016.
[58] W. Zhang, Y. Zhu, Q.Y. Zhang, L. Ma, L. Yang, W. Guo, G. Ge, Research progress in application and mechanism of Schisandrae Chinensis Fructus for prevention and treatment of liver diseases, China J. Chin. Mater. Med. 45 (16) (2020) 3759–3769, https://doi.org/10.19540/j.cnki.cjcmm.20200513.601.
[59] X.Y. Wang, Z.L. Yu, S.Y. Pan, Y. Zhang, N. Sun, P.L. Zhu, Z.H. Jia, S.F. Zhou, K.M. Ko, Supplementation with the extract of schisandrae fructus pulp, seed, or their combination influences the metabolism of lipids and glucose in mice fed with normal and hypercholesterolemic diet, Evid. Based Complement, Alternat. Med. (2014), 472638, https://doi.org/10.1155/2014/472638, 2014.
[60] Y.F. Zhou, M. Niu, J.X. Fang, Y.Q. Ma, Y.Y. Cui, Y. Dong, R.R. Zhang, J.B. Wang, P. Zhang, Metabonomics study on hepatoprotective effect of Schisandrae Chinensis Fructus based on UPLC-Q-TOF-MS, China J. Chin. Mater. Med. 43 (18) (2018) 3756–3763, https://doi.org/10.19540/j.cnki.cjcmm.20180516.004.